ราชวิทยาลัย จุฬาภรณ์

The Journal of Chulabhorn Royal Academy

eISSN : 3027-7418 (Online)

Research article

Utility of 18F-FDG PET/CT Combined With Dedicated Brain PET/MRI in Determination Of Brain Metastasis From Lung Cancer

Supanida Mayurasakorn, Dheeratama Siripongsatian, Anchisa Kunawudhi, Chetsadaporn Promteangtrong, Peerapon Kiatkittikul, Attapon Jantarato, Chanisa Chotipanich*

National Cyclotron and PET Centre, Chulabhorn Hospital

*Corresponding author, email: chanisa.cho@cra.ac.th

Received: 26 March 2023; Revised: 11 October 2024; Accepted: 15 October 2024

Abstract

Background and Purpose: Diagnosing brain metastasis is important in managing lung cancer. We compared ^{18}F-FDG PET/CT combined with dedicated brain PET/MRI and ^{18}F-FDG PET/CT alone in diagnosing brain metastasis from lung cancer and investigated the quantitative parameters affecting the positivity of PET scans. **Methods:** This study included 89 patients (age: 43–88 years; 58% men) with pathologically confirmed lung cancer who underwent whole-body ^{18}F-FDG PET/CT and dedicated brain PET/MRI with gadolinium contrast enhancement. Imaging data acquired between October 2020 and February 2021 were retrospectively collected, and MRI findings were used as the reference standard for diagnosing brain metastasis. The detection of brain metastasis was compared between ^{18}F-FDG PET/CT alone and ^{18}F-FDG PET/CT combined with dedicated brain PET/MRI. Quantitative parameters were analyzed to determine factors affecting the positivity of the PET scan results. Correlations between these quantitative parameters were also examined. **Results:** Per-patient and per-lesion detection of brain metastasis on PET/CT alone versus that combined with dedicated brain PET/MRI with gadolinium contrast enhancement showed ratios of 0.64 and 0.17, respectively. Quantitative parameters with the highest areas under the curve from receiver operating characteristics analysis were the maximum tumor-to-background ratio and the size of the metastasis. The optimum maximum tumor-to-background ratio cut-off, with the highest area under the curve, for PET positivity was 1.83. The minimum and mean lesion sizes for detection on PET were 0.3 cm and 1.45 cm, respectively. **Conclusions:** PET/MRI can augment the detection of brain metastasis from lung cancer compared with PET/CT alone. High FDG background activity in the brain parenchyma may hinder the positivity of PET results. Therefore, MRI is important for detecting brain metastasis.

Keywords: Brain metastasis, ^{18}F-FDG, lung cancer, PET/CT, PET/MRI

Introduction

Lung cancer is a substantial cause of morbidity and mortality. In 2020, the World Health Organization ranked lung cancer as the second most common malignancy type causing mortality worldwide[1]. One of important sites of lung cancer metastasis is the brain. A study reported that 10.4% of patients with lung cancer had brain metastasis at the time of their diagnosis[2]. Despite asymptomatic cases and the advancement of targeted therapies, such as tyrosine kinase inhibitors, radiotherapy treatment is still suggested in some

© Chulabhorn Royal Academy. Terms and conditions of Creative Commons Attribution 4.0 International (CC BY NC ND 4.0) apply

patients. There has been a decreasing role for whole-brain radiotherapy because of its potential long-term neurocognitive effects[3]. Stereotactic radiosurgery is an option for those with oligometastasis in the brain[3,4,5]. Therefore, the efficacy of imaging is crucial for optimal surgical planning. Additionally, thorough screening for metastasis from lung cancer can reduce the number of unnecessary invasive procedures without a cure, such as thoracotomy, and their associated costs[2,6-8].

Computed tomography (CT) of the chest and other parts of the body is the imaging technique of choice for diagnosing metastases. ^{18}F-fluorodeoxyglucose (FDG) positron emission tomography (PET) combined with CT provides better information on lesion metabolism and anatomy than a PET scan or CT alone, especially in the detection of extrathoracic metastasis[9-17]. PET imaging also provides details about tumor physiology, which is a unique aspect of its nature as functional imaging. Nevertheless, the efficacy of ^{18}F-FDG PET/CT for detecting brain metastasis, which is hindered by high FDG background activity, may be lower than that of brain MRI[9-11,16,18-19]. MRI is the current gold standard, but it might not be widely available and has limitations in the cases of patients with implanted devices and in claustrophobic patients. Gadolinium contrast agent used in MRI might also be contraindicated in some patients with poor renal function owing to nephrogenic systemic fibrosis.

In this study, we compared ^{18}F-FDG PET/CT combined with dedicated brain PET/MRI and ^{18}F-FDG PET/CT alone in the diagnosis of brain metastasis. Additionally, we evaluated the quantitative PET parameters that affect positivity in the visual imaging analysis.

Methods

This retrospective study was approved by the Human Research Ethics Committee of Chulabhorn Research Institute (IRB no. 127/2564). We included data from patients with pathologically confirmed lung cancer who underwent ^{18}F-FDG PET/CT with dedicated brain PET/MRI at our center between October 2020 and February 2021. The exclusion criteria were as follows: (1) neurological symptoms suggestive of brain metastasis, (2) a history of any type of cranial surgery, (3) a history of other primary malignancies, and (4) a lack of pathological results for primary lung cancer.

^{18}F-FDG PET/CT and dedicated brain PET/MRI were performed on the same day. All patients fasted for at least 8 hours before scanning and had a serum glucose concentration no higher than 180 mg/dL. All ^{18}F-FDG PET/CT whole-body procedures were performed using a 64-slice Siemens Biograph scanner (Siemens Healthineers GmbH, Erlangen, Germany) 60 minutes after the ^{18}F-FDG was injected intravenously. The dose of radiopharmaceuticals was calculated according to the following equation: 2.59 MBq×body weight (kg). A three-dimensional emission scan was performed from the vertex to the proximal thighs with continuous bed motion over 10 minutes. Noncontrast CT imaging was also performed from the vertex to the proximal thighs for the correction of attenuation and structural images. The reconstruction parameters for attenuation correction images were ultra-high-definition PET (point spread function and time of flight) with two iterations and five subsets, an image size of 440×440, all pass filters, and a zoom factor of 1. The PET data were reconstructed into whole-body static images.

^{18}F-FDG PET/MRI of the brain was performed after whole-body acquisition on a simultaneous PET-MRI 3 Tesla scanner (Siemens Healthcare GmbH, Erlangen, Germany) approximately 70 minutes after an intravenous injection of 2.59 MBq/kg of ^{18}F-FDG. Single-bed PET dynamic list-mode acquisition was carried out simultaneously with MRI acquisition. The DIXON high-resolution brain sequence was used, with a voxel size of 1.3×1.3×2.0 mm, an echo time of 1.28/2.51 ms, and a repetition time of 4.14 ms. A five-compartment segmentation (air, water, lung, adipose tissue, and bone) was used. Various MRI sequences were applied, including sagittal T1 three-dimensional, axial diffusion-weighted imaging with b0 and b1000, axial T2-weighted fluid-attenuated inversion recovery with fat suppression, axial susceptibility-weighted imaging, and coronal T2-weighted images. An axial T1-weighted volumetric interpolated breath-hold examination was performed before gadolinium enhancement. Contrast-enhanced

MRI was performed with 10–15 mL (0.2 mL/kg) of gadolinium at an injection rate of 2 mL/s. Clinicians did not use gadolinium contrast in patients with a history of gadolinium hypersensitivity or impaired renal function (glomerular filtration rate <45 mL/minute). This procedure was followed by an axial T-1 weighted volumetric interpolated breath-hold examination and sagittal T1 three-dimensional imaging with fat suppression. PET data were reconstructed using the following parameters: point spread function of high-definition PET with 6 iterations and 21 subsets, matrix size=512×512, zoom=2, and an all-pass filter. The data were interpreted using the MM oncology workflow of the Syngovia workstation (Siemens Healthineers).

PET imaging was interpreted by at least two nuclear medicine physicians. CT and MRI imaging were interpreted by diagnostic radiologists. The experience of the interpreters ranged from 3 to more than 10 years. Pathological confirmation of the brain lesions was not performed for ethical reasons.

The detection rates of PET/CT compared with PET/MRI were calculated in per-patient and per-lesion analyses. PET and MRI parameters, such as lesion size, specific uptake value (SUV), metabolic tumor volume (MTV), total lesion glycolysis (TLG), and apparent diffusion coefficient (ADC), were calculated automatically from the same volume of interest (VOI) using Syngovia software. The VOI was selected according to the anatomical images from the MRI.

The maximum tumor-to-background ratio (TBRmax) was calculated as the maximum SUV of the tumor VOI divided by the mean background activity in the normal contralateral hemisphere. The mean TBR (TBRmean) was calculated as the mean SUV of the tumor VOI divided by the mean background activity in the normal contralateral hemisphere. The standardized uptake value ratio (SUVR) was calculated as the maximum SUV of the tumor VOI divided by the mean background activity in the normal contralateral cerebellum. Quantitative PET and MRI parameters calculated from the same VOI were compared between patients who were positive and negative for brain metastasis on PET imaging.

A logistic regression analysis was performed to determine the associations between the parameters and the positivity of the PET imaging. Receiver operating characteristics (ROC) analysis was also carried out. The degree of correlation between these quantitative parameters was assessed using Spearman's rank correlation. P values <0.05 indicated statistical significance.

Results

Eighty-nine patients were included in the study. The patients' ages ranged from 43 to 88 years, with a median age of 66 years. Fifty-two (58%) patients were men.

The indication for scanning was initial staging in 76 (85%) patients. Some patients underwent scans for restaging and workup because of disease recurrence. In the group of patients sent for initial staging, 47% had no extrathoracic metastasis. However, 53% of the patients had extrathoracic metastasis. Lymph nodes were the most common site, followed by bones and the brain. Isolated brain metastasis accounted for 6.6% of patients sent for initial staging. Brain MRI was used as the reference standard for the diagnosis of brain metastasis. The detection rate was calculated only for PET/CT because there were no false-negative results for brain MRI.

In the per-patient analysis, there were 14 patients with brain metastases, all of whom showed positive lesions on the brain MRI. However, PET/CT enabled the detection of brain metastases in only nine (64%) of these patients. The other five (36%) patients showed negative results. An example of a positive case is shown in Figure 1.

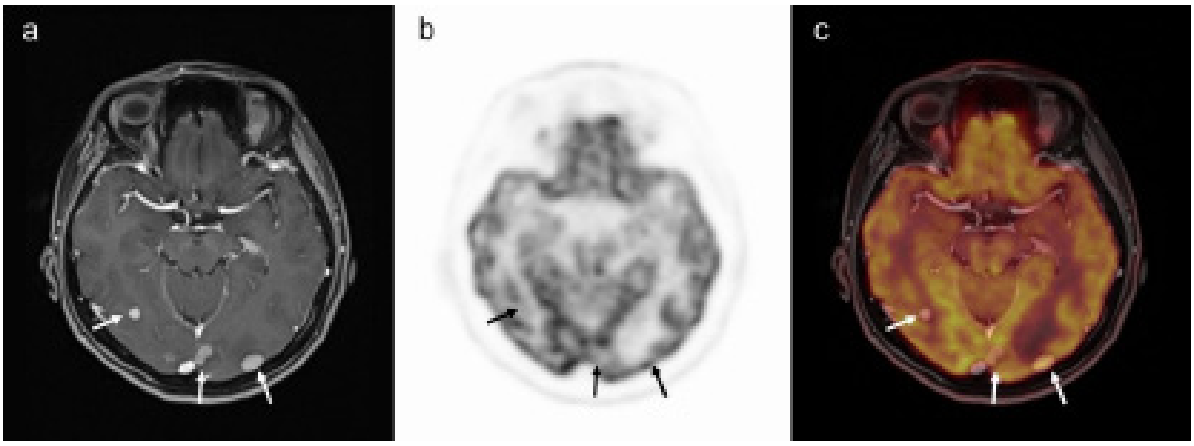


Figure 1 Images of a 63-year-old woman with lung cancer who was sent for restaging after lobectomy and chemotherapy in 2019. (A) Axial T1-weighted image with gadolinium enhancement shows multiple enhancing nodules scattered over the bilateral cerebral hemispheres. (B) and (C) Attenuation-corrected axial ^{18}F-FDG PET and fused axial ^{18}F-FDG PET images of the same plane show no abnormal hypermetabolic uptake beyond that of the normal brain parenchyma.

In the per-lesion analysis, 81 brain metastatic lesions were detected on brain MRI, of which only 14 (17.3%) were detected on PET. The remaining 67 lesions were undetected. The quantitative PET parameters calculated from PET/MRI images in patients who showed positive and negative results for brain metastasis on PET imaging are shown in Table 1.

Table 1 Comparison of quantitative parameters of metastatic lesions detected on PET and those not detected on PET.

Parameter		Lesions that were positive on PET (n=14)	Lesions that were negative on PET (n=67)
Lesion size (cm)	Mean	1.45	0.45
	Max/Min	3.6/03	1.4/0.16
	Median	1.3	0.4
	IQR	0.93–1.42	0.3–0.5
SUVmax	Mean	15.04	11.11
	Max/Min	30.12/8.43	17.08/6.66
	Median	14.35	10.88
	IQR	10.92–16.79	8.97–12.84
SUVmean	Mean	9.49	8.1
	Max/Min	20.21/4.5	12.37/4.66
	Median	9.32	8.21
	IQR	6.6–10.74	6.81–8.78

SUVpeak	Mean	8.14	7.84
	Max/Min	16.2/3.31	11.51/5.2
	Median	8.16	7.84
	IQR	6.97–8.69	6.59–8.78
TLG	Mean	20.66	2.25
	Max/Min	171.55/1.39	14.9/0.18
	Median	8.16	1.36
	IQR	4.28–13.33	0.98–2.53
MTV	Mean	2.1	0.28
	Max/Min	12.18/0.08	2.23/0.02
	Median	0.87	0.17
	IQR	0.5–1.63	0.12–0.29
TBRmax	Mean	2.67	1.5
	Max/Min	5/1.63	3.4/1.08
	Median	2.35	1.4
	IQR	1.98–3.0	1.3–1.6
TBRmean	Mean	2.67	1.5
	Max/Min	5/1.63	3.4/1.08
	Median	2.35	1.4
	IQR	1.98–3.0	1.3–1.6
TBRmean	Mean	1.66	1.1
	Max/Min	3.36/1.06	2.8/0.84
	Median	1.4	1.1
	IQR	1.23–1.9	0.96–1.15
SUVR	Mean	2.73	1.62
	Max/Min	5.45/1.09	2.3/0.98
	Median	2.37	1.64
	IQR	1.97–3.38	1.37–1.87
Mean ADC	Mean	998.35	839.48
	Max/Min	1285.04/698	1088/589.5
	Median	909.5	817.8
	IQR	831.73–1224.5	759.5–931.1

The detection rate of the per-lesion analysis was 0.17. IQR, interquartile range; SUV, standardized uptake value; TLG, total lesion glycolysis; MTV, metabolic tumor volume; TBR, tumor-to-background ratio; SUVR, standardized uptake value ratio; ADC, apparent diffusion coefficient.

The logistic regression and ROC analyses of quantitative parameters from the 81 detected brain metastatic lesions that could affect the positivity of the PET component of PET/MRI are shown in Table 2. A multivariate

logistic regression analysis could not be performed because of the inadequate number of positive lesions (only 14 lesions). Therefore, only crude odds ratio values from the univariate analysis were reported. Multicollinearity between the parameters was also found, which resulted in a wide range of 95% confidence intervals.

In the ROC analysis, TBRmax and lesion size were the parameters with the highest area under the curve (AUC) for differentiating negative and positive lesions on PET imaging. The optimum TBRmax cutoff with the highest AUC for PET positivity was 1.83.

Table 2 Univariate logistic regression analysis and area under the ROC curve for each quantitative PET parameter.

Parameter	Univariate analysis		Area under the ROC curve (95% CI)
	Crude OR (95% CI)	P value	
TBRmax	69.3 (6.8–708.4)	<0.001	0.96 (0.92–1.00)
Lesion size	100.7 (11.9–848.2)	<0.001	0.92 (0.83–1.00)
TLG	1.4 (1.2–1.7)	<0.001	0.89 (0.80–0.98)
TBRmean	29.9 (2.9–309.8)	0.004	0.87 (0.76–0.97)
MTV	10.7 (2.5–45.9)	0.001	0.83 (0.69–0.98)
SUVR	18.1 (2.9–110.2)	0.002	0.81 (0.63–0.99)
SUVmax	1.34 (1.09–1.65)	0.006	0.73 (0.56–0.89)
Mean ADC	1.01 (1.00–1.01)	0.002	0.72 (0.55–0.88)
SUVmean	1.25 (0.98–1.59)	0.068	–
SUVpeak	1.09 (0.81–1.47)	0.579	–

TBRmax and the size of the lesion had the highest crude ORs and AUCs. P<0.05 indicates statistical significance.

Only significant parameters from the logistic regression analysis underwent Spearman's correlation analysis. Lesion size showed a strong significant correlation with TLG and MTV and a weak-to-moderate correlation with SUVmax, SUVR, TBRmax, and the mean ADC value. There was a strong correlation between TBRmax and TBRmean (Table 3).

Spearman's rho (P value)	Size	SUV max	TLG	MTV	TBR max	TBR mean	SUVR	Mean ADC value
Lesion size	1.0							
SUVmax	0.28 (0.01)	1.0						
TLG	0.75 (<0.001)	0.51 (<0.001)	1.0					

MTV	0.75 (<0.001)	0.23 (0.04)	0.93 (<0.001)	1.0				
TBRmax	0.4 (<0.001)	0.33 (0.003)	0.44 (<0.001)	0.4 (<0.001)	1.0			
TBRmean	0.1 (0.4)	0.17 (0.13)	0.18 (0.13)	0.15 (0.2)	0.83 (<0.001)	1.0		
SUVR	0.35 (0.001)	0.85 (<0.001)	0.56 (<0.001)	0.32 (0.003)	0.44 (<0.001)	0.26 (0.02)	1.0	
Mean ADC value	0.36 (0.001)	0.34 (0.002)	0.33 (0.003)	0.26 (0.2)	0.11 (0.34)	−0.07 (0.5)	0.32 (0.004)	1.0

P <0.05 indicates statistical significance.

Discussion

Additional detection of brain metastasis by dedicated brain PET/MRI

In the patient-based analysis, the detection of brain metastasis by PET/CT alone had a ratio of 0.64 per patient compared with MRI as the reference standard, which is higher than that reported in previous studies[19-21]. A comparison of the sensitivity of PET/CT for detecting brain metastasis in our study and in previous studies is shown in Table 4.

Table 4 Sensitivity for the diagnosis of brain metastasis on PET/CT compared with dedicated brain MRI or PET/MRI in previous studies.

Study	Origin	Study type	No. of patients	No. of patients positive for brain metastasis	Contrast -enhanced CT	MRI	PET/CT sensitivity (%)	Brain MRI sensitivity (%)a
Kruger et al.	Germany	Prospective	104	22	Yes	1.5 T	27.3% (6/22)	-
Lee et al.	Korea	Prospective	442	50	No	3 T	24% (12/50)	88
Ho et al.	Taiwan	Retrospective	805	79	No	3 T	27% (21/79)	-
This study	Thailand	Retrospective	89	14	No	3 T	64% (9/14)	-

[a]Brain MRI sensitivity was not available for some studies because MRI was used as the reference standard.

In the per-lesion analysis, the detection rate of PET/CT was relatively low (0.17). The reason for this finding may be that some patients had both positive and negative PET brain metastasis. Small lesions may not have been detected, although these patients were still considered positive cases in the per-patient analysis. This fact, along with other potential differences, such as fewer patients with brain metastases and different scanners, might have resulted in more positive cases in our per-patient analysis than in other previous studies. The improved brain metastasis detection rate achieved with dedicated brain PET/MRI appears to be necessary to supplement standard PET/CT for detecting brain metastasis.

Quantitative parameters associated with positivity of PET and correlations between parameters.

Following univariate logistic regression and ROC analysis, quantitative PET parameters which affected the positivity of lesions on the PET imaging with an AUC of >0.8 were TBRmax, size, TLG, TBRmean, MTV, and SUVR. The high AUCs reflected their potential to differentiate between negative and positive lesions on PET imaging When a lesion was large and the uptake of FDG was high compared with relatively high background activity in the brain, the lesion was more visible. However, the TBRmean might not be an ideal parameter for differentiating between the positivity and negativity of lesions. The reason for this could be because some lesions had low central FDG uptake and TBRmean values, even though the lesions were clearly visible (Figure 2).

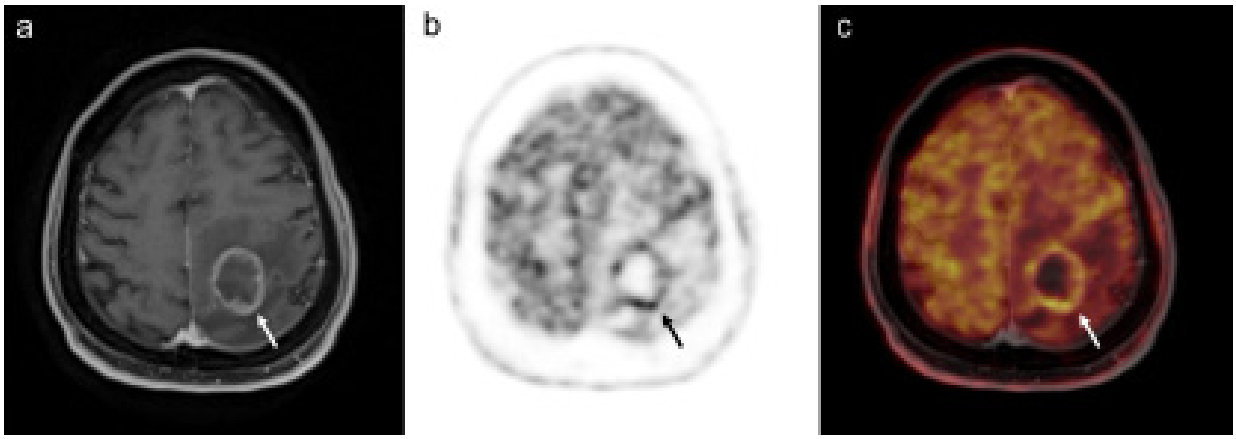


Figure 2 Images of a 62-year-old man with lung cancer who was sent for initial staging: (A) Axial T1-weighted image with gadolinium enhancement shows a 3-cm ring-enhancing lesion in the left frontoparietal region. (B) and (C) Attenuation-corrected axial ^{18}F-FDG PET image and fused axial 18F-FDG PET image of the same plane with increased ^{18}F-FDG uptake at the periphery of the lesion and low central 18F-FDG uptake, resulting in a low TBRmean value.

The most important findings related to the quantitative parameters involved TBRmax and lesion size. The lesion size was related to the positivity of the PET images, which is similar to the results of a study conducted by Deuschl et al. in 2017[11]. In 2019, Ho et al.[21] reported that the minimum and mean sizes of positive PET lesions were 0.6 cm and 1.8±1.2 cm, respectively. These sizes are slightly different from our results of 0.3 cm and 1.45 cm, respectively. Regarding TBRmax, Ho et al. reported that the mean and minimum TBRmax values of lesions positive on PET were 2.6±0.8 and 1.6, respectively. In our study, no lesions with a TBRmax <1.6 were positive on PET. Additionally, we found that the TBRmax cut-off point at which all PET scans should be positive was 1.83, which had optimum sensitivity and specificity, as shown by the ROC analysis.

However, 4 of the 17 lesions with a TBRmax >1.83 were negative on PET. This finding may be explained by the small size of some lesions, causing difficulty in selecting the region of interest. Additionally, the lesion sites were near the cortex of the brain, where the TBRmax values may have been exaggerated.

The correlation analysis between the quantitative parameters showed a strong correlation between lesion size and TLG and MTV, which is consistent with the fact that lesion size can directly affect TLG and MTV values in the formulas. However, there was a poor correlation between the ADC values and the FDG PET parameters. This finding suggests that the cellularity of brain metastasis from lung cancer has no association with tumor glucose metabolism.

In summary, PET/MRI provided improved detection of brain metastasis compared to PET/CT alone, and the MRI was the main component of this result. Besides controllable factors, such as blood glucose, the detection of brain metastasis in PET imaging is hindered by high physiological background activity. Currently, this problem has no definite solution. An adequate tumor-to-background ratio and size were required to visually detect the lesions. If a lesion is detected, positive FDG uptake of the lesion could reflect useful information on tumor biology. PET/CT showed false-negative results for brain metastasis of up to 33% in the per-patient analysis and up to 83% in the per-lesion analysis. Therefore, dedicated brain MRI or PET/MRI should still be considered in high-risk patients, depending on local availability. The limitations of this study include the small sample size and the lack of a long-term follow-up. A longer follow-up may yield information on the effects of these investigations on patient outcomes, such as the survival benefit.

Conclusion

PET/CT alone showed relatively high false-negative results for brain metastasis compared with PET/MRI. Therefore, dedicated brain MRI or PET/MRI in addition to the standard PET/CT protocol should be considered in high-risk patients with negative PET/CT findings. The most important parameters in differentiating between negative and positive lesions on PET imaging are TBRmax and lesion size.

Acknowledgements

We thank Ellen Knapp, PhD, from Scribendi (www.scribendi.com) for editing a draft of this manuscript.

References

1. Sung H, Ferlay J, Siegel RL, et al. Global Cancer Statistics 2020: GLOBOCAN Estimates of Incidence and Mortality Worldwide for 36 Cancers in 185 Countries. *CA Cancer J Clin*. 2021;71(3):209-249. doi:10.3322/caac.21660
2. Investigating extrathoracic metastatic disease in patients with apparently operable lung cancer. The Canadian Lung Oncology Group. *Ann Thorac Surg*. 2001;71(2):425-434.
3. Vogelbaum MA, Brown PD, Messersmith H, et al. Treatment for Brain Metastases: ASCO-SNO-ASTRO Guideline [published correction appears in J Clin Oncol. 2022 Apr 20;40(12):1392. doi: 10.1200/JCO.22.00593]. *J Clin Oncol*. 2022;40 (5):492-516. doi:10.1200/JCO.21.02314
4. National Comprehensive Cancer Network (NCCN). NCCN Clinical Practice Guidelines in Oncology. Non-Small Cell Lung Cancer Version7. 2021. https://www.nccn.org/professionals/physician_gls/pdf/nscl.pdf. Accessed November 10, 2021.
5. Ernani V, Stinchcombe TE. Management of Brain Metastases in Non-Small-Cell Lung Cancer [published correction appears in JCO Oncol Pract. 2020 Mar;16(3):149. doi: 10.1200/JOP.20.00042]. *J Oncol Pract*. 2019;15(11): 563-570. doi:10.1200/JOP.19.00357
6. van Tinteren H, Hoekstra OS, Smit EF, et al. Effectiveness of positron emission tomography in the preoperative assessment of patients with suspected non-small-cell lung cancer: the PLUS multicentre randomised trial. *Lancet*. 2002;359(9315):1388-1393. doi:10.1016/s0140-6736(02)08352-6
7. Gambhir SS, Hoh CK, Phelps ME, Madar I, Maddahi J. Decision tree sensitivity analysis for cost-effectiveness of FDG-PET in the staging and management of non-small-cell lung carcinoma. *J Nucl Med*. 1996;37(9):1428-1436.
8. Chao F, Zhang H. PET/CT in the staging of the non-small-cell lung cancer. *J Biomed Biotechnol*. 2012;2012:783739. doi:10.1155/2012/783739
9. Brink I, Schumacher T, Mix M, et al. Impact

of [18F]FDG-PET on the primary staging of small-cell lung cancer. *Eur J Nucl Med Mol maging*. 2004;31(12):1614-1620. doi:10.1007/s00259-004-1606-x

10. Steinert HC. PET and PET-CT of lung cancer. *Methods Mol Biol*. 2011;727:33-51. doi:10.1007/978-1-61779-062-1_3
11. Deuschl C, Nensa F, Grueneisen J, et al. Diagnostic impact of integrated 18F-FDG PET/MRI in cerebral staging of patients with non-small cell lung cancer. *Acta Radiol*. 2017;58(8):991-996. doi:10.1177/0284185116681041
12. De Wever W, Stroobants S, Coolen J, Verschakelen JA. Integrated PET/CT in the staging of nonsmall cell lung cancer: technical aspects and clinical integration. *Eur Respir J*. 2009;33(1):201-212. doi:10.1183/09031936.00035108
13. Lardinois D, Weder W, Hany TF, et al. Staging of non-small-cell lung cancer with integrated positron-emission tomography and computed tomography. *N Engl J Med*. 2003;348(25):2500-2507. doi:10.1056/NEJMoa022136
14. De Wever W, Ceyssens S, Mortelmans L, et al. Additional value of PET-CT in the staging of lung cancer: comparison with CT alone, PET alone and visual correlation of PET and CT. *Eur Radiol*. 2007;17(1):23-32. doi:10.1007/s00330-006-0284-4
15. De Wever W, Vankan Y, Stroobants S, Verschakelen J. Detection of extrapulmonary lesions with integrated PET/CT in the staging of lung cancer. *Eur Respir J*. 2007;29(5):995. doi:10.1183/09031936.00119106
16. Wu Y, Li P, Zhang H, et al. Diagnostic value of fluorine 18 fluorodeoxyglucose positron emission tomography/computed tomography for the detection of metastases in non-small-cell lung cancer patients. *Int J Cancer*. 2013;132(2):E37-E47. doi:10.1002/ijc.27779
17. Cerfolio RJ, Ojha B, Bryant AS, Raghuveer V, Mountz JM, Bartolucci AA. The accuracy of integrated PET-CT compared with dedicated PET alone for the staging of patients with nonsmall cell lung cancer. *Ann Thorac Surg*. 2004;78(3):1017-1023. doi:10.1016/j.athoracsur.2004.02.067
18. Weder W, Schmid RA, Bruchhaus H, Hillinger S, von Schulthess GK, Steinert HC. Detection of extrathoracic metastases by positron emission tomography in lung cancer. *Ann Thorac Surg*. 1998;66(3):886-893. doi:10.1016/s0003-4975(98)00675-4
19. Krüger S, Mottaghy FM, Buck AK, et al. Brain metastasis in lung cancer. Comparison of cerebral MRI and 18F-FDG-PET/CT for diagnosis in the initial staging. *Nuklearmedizin*. 2011;50(3):101-106. doi:10.3413/Nukmed-0338-10-07
20. Lee HY, Lee KS, Kim BT, et al. Diagnostic efficacy of PET/CT plus brain MR imaging for detection of extrathoracic metastases in patients with lung adenocarcinoma. *J Korean Med Sci*. 2009;24(6):1132-1138. doi:10.3346/jkms.2009.24.6.1132
21. Ho KC, Toh CH, Li SH, et al. Prognostic impact of combining whole-body PET/CT and brain PET/MR in patients with lung adenocarcinoma and brain metastases. *Eur J Nucl Med Mol Imaging*. 2019;46(2):467-477. doi:10.1007/s00259-018-4210-1

การอ้างอิง

Mayurasakorn S., Siripongsatian D., Kunawudhi A., Promteangtrong C., Kiatkittikul P., Jantarato A., Chotipanich C. Utility of 18F-FDG PET/CT Combined With Dedicated Brain PET/MRI in Determination Of Brain Metastasis From Lung Cancer. J Chulabhorn Royal Acad. 2024; 6(3): 169-178. https://he02.tci-thaijo.org/index.php/jcra/article/view/262025

Online Access

https://he02.tci-thaijo.org/index.php/jcra/article/view/262025